Mem. S.A.It. Vol. 83, 259
© SAIt 2012
Memorie della

Giant radio pulses of the Crab Pulsar

A multifrequency study

N. Lewandowska[1], C. Wendel[1], V. Kondratiev[2], D. Elsaesser[1], and K. Mannheim[1]

[1] University of Wuerzburg, Lehrstuhl fuer Astronomie, Emil-Fischer Strasse 31, 97074 Wuerzburg
[2] ASTRON, Oude Hoogeveensedijk 4, 7991 PD Dwingeloo, The Netherlands e-mail: Natalia.Lewandowska@physik.uni-wuerzburg.de

Abstract. Giant pulses (GPs) are a special form of radio emission observed from the Crab pulsar. They differ from regular pulses by their sporadic occurence mainly at the phases of the main pulse (P1) and the interpulse (P2), their flux densities which are at least by a factor of 1000 higher in contrast with regular pulses and their pulse widths ranging from nano- to microseconds. Several theories have been developed regarding the possible origin and properties of Crab radio GPs. One of them refers to the generation of GPs on closed magnetic field lines via reconnection events near the light cylinder. Recent detections of high energy flares originating apparently from the Crab nebula give rise to the question for the energy reservoir to power these outbursts detected by AGILE and Fermi LAT in 2010. Testing the theory of reconnection zones being probably responsible for the appearance of radio GPs and simultaneaously the energy reservoir for the observed flares, we examine the characteristics of radio GPs taken with the Westerbork Synthesis Radio Telescop (WSRT) after the Crab nebula flare 2010.
Simultaneously we examine the energetics of the 2010 flare event by photometrical studies of HST images of the anvil region.

Key words. Crab pulsar – neutron stars – pulsars – giant pulses – regular pulses – magnetic field – flux densities

1. Introduction

1.1. Radio Giant Pulses

Among the already over 1500 known pulsars, the Crab pulsar still represents an extraordinary object. It is the only pulsar known so far with a pulsed emission profile visible over the entire electromagnetic spectrum from radio to GeV energies. Its regular pulse structure reveals several implementations. Beginning with a precursor pulse which is only visible at a frequency range from ≈ 300 to 600 MHz, two more prominent pulses, known as the main pulse and the interpulse, follow at the phases of 70 and ≈ 110 degrees. In addition two higher frequency components, known as HFC1 and HFC2, appear at a frequency range from ≈ 4000 to 8000 MHz simultaneaously with a phase shift of the interpulse by about 10 degrees (Moffett & Hankins (1996)).

Send offprint requests to: N.Lewandowska

In this regular pulse profile GPs represent a rather exotic form of pulsar radio emission. Occuring mainly at the phases of P1 and P2, they exhibit flux densities higher by a factor of 5 x 10^5, pulse widths from 1 - 2 microseconds and their apparently non periodical appearance (Kuzmin (2007)).
Their occurence was verified in a wide frequency range from 23 MHz (Popov et al. (2006)) to 15.1 GHz (Hankins (2000), Jessner et al. (2010)) at the phases of P1 and P2. Further studies reveal the existence of GPs also at both HFC components (Jessner et al. (2005), Hankins (2000)), although none could be verified at the phase of the precursor until now. Hence their appearance is apparently phase bounded.
A further unexpected property of GPs was discovered by Hankins & Eilek (2007). They confirmed the detection of different time and frequency patterns of the GPs occuring at P1 and at P2 at frequencies above 4 GHz. While GPs occuring at P1 consists of narrow-band pulses of nanoseconds duration, GPs occuring at the phase of P2 reveal narrow emission bands which have typical durations in the microseconds range. The different structures of GPs at P1 and P2 imply probable different emission mechanisms which lead to the development of both regular pulse structures. This on the other hand contradicts previous emission theories of the Crab pulsar which refer to a similar emission mechanism of P1 and P2.
In spite of over 40 years of observations and the detection of the Crab pulsar by its GPs (Staelin & Reifenstein (1968)), the origin and properties of GPs are still not understood. Several theories have been established to describe the occurence and characteristics of GPs (Mikhailovskii et al. (1985), Weatherall (2001), Hankins (2003), Petrova (2004), Istomin (2004)).
The emission bands of giant interpulses (GIP) detected by Hankins & Eilek (2007) were reconstructed by the Lyutikov model (Lyutikov (2007)). According to this a higher particle density exists on closed magnetic field lines in contrast with the standard Goldreich-Julian model. Under the assumption that this density is highest near the last closed magnetic field line, a Lorenz beam developes through magnetic reconnection events. It moves along the respective closed field line and dissipates by curvature radiation. However, this model refers only to GIPs above 4 GHz. Currently no general model for the origin of Crab GPs exists.
The GP emission has also been detected in the case of other pulsars. Altogether 11 pulsars which emit GPs are known consisting of young pulsars like the Crab and millisecond pulsars (MSP) (Slowikowska et al. (2007)). A common feature of all such pulsars was thought to be a high magnetic field. Nevertheless a uniform accordance in all known GP emitting pulsars could not be found.
The GP phenomenon remains therewith widely not understood up until today.

1.2. Multiwavelength observations

To understand the emission mechanism of Crab GPs, several multiwavelength (MWL) campaigns were carried out. Since all these observation campaigns could neither prove a correlation between radio GPs and X-ray photons (Lundgren et al. (1995)), nor between radio GPs and γ photons (Bilous et al., 2009, 2010, 2011), the opinion of GPs caused solely by coherent emission processes arose.
However, in one case a correlation could be verified. Shearer et al. (2003) observed the Crab simultaneaously with the WSRT and the optical photometer TRIFFID. They provided evidence that the brightness of optical pulses is higher by $\approx$ 3 % during occuring radio GPs. Hence an additional non-coherent emission process is probably responsible for the GP emission mechanism which releases energy in wide parts of the electromagnetic spectrum.
Currently it is assumed that Crab GPs can be caused by coherent radio emission, pair production in the magnetosphere, or changes of the beaming direction. Further MWL studies are needed to explore the emission processes standing behind this kind of extraordinary radio pulses.

1.3. Crab Nebula Flares

Since February 2007 several flares coming from a region in the Crab nebula were detected by AGILE, Fermi and several other observatories (Abdo et al. (2011)).
Regarding the flare from September 2010 (Tavani et al. (2010)) we carried out an optical analysis with three Hubble Space Telescope (HST) exposures gained from the HST archive [1]. The analysis refers to the determination of the synchrotron emission power of the anvil region which is located about 10 arcseconds away from the Crab pulsar and in which a rise of brightness was observed after the flare in September 2010.
Under the assumption that the whole Crab nebula is powered only by the pulsar, a brightness increase of this kind puts in question how it affects the rotation and the energetics of the latter. Due to their characteristics radio GPs depict possible indicators for changes in the parameters of the pulsar if a connection between these extraordinary radio pulses which are apparently invoked by magnetic reconnection events near the light cylinder and the rather sporadically occuring Crab nebula flares exist.

2. Observations

2.1. Radio Observations

All radio observations were carried out with the Westerbork Synthesis Radio Telescope (WSRT) at a frequency of 1.38 GHz in a phased array mode. With the help of the open source pulsar data processing software package DSPSR[2] and the dispersion measure provided by Jodrell Bank[3] the data was coherently dedispersed.
As already mentioned all GPs occur aligned in phase with regular pulses (Figure 1). To filter them out from the regular pulses, the treshold was set up to 7 σ which results in over 1500 GPs (Figure 2).
To assign definite flux values to each single GP, the whole data set was flux calibrated with the

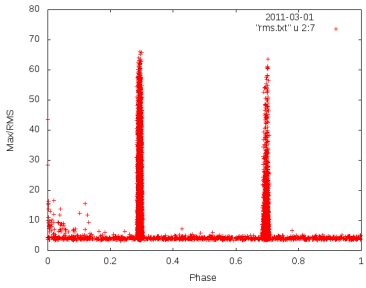

Fig. 1. Phase diagram of all pulses observed with the WSRT on March 1th 2011

modified radiometer equation (**?**).
The following part of the analysis several characteristics of the observed radio GPs are extracted and compared with already published values. Referring to Karuppusamy et al. (2010) one GP appears every 0.803 seconds. A change in the GP rate might be a possible hint for a contribution of the pulsar in the observed flares.
Apart from this the pulse energy distribution and pulse widths are examined. It is known that the intensity distribution of GPs follow a power law (Argyle et al. (1972)) in contrast with regular pulses whose intensities are Gaussian distributed (Hesse et al. (1974)). In this analysis we extract the brightest ones which contribute to the power law tail of the distribution in search for a possible decrease. Besides it has been observed that short width GPs have the highest flux densities (Sallmen et al. (1999), Hankins (2003)). A test of the width distribution of all detected GP in our data set will provide further insight into a variation of their fluxes.

2.2. Optical Observations

For our analysis three exposures taken with the HST in combination with the ACS camera and the F550M filter[4] were selected in which the anvil region was defined as a spherical shape with a radius of 0.034 pc. The frequency-dependent synchrotron emis-

[1] http://archive.eso.org/archive/hst/
[2] http://dspsr.sourceforge.net/
[3] http://www.jb.man.ac.uk/~pulsar/crab.htm
[4] http://acs.pha.jhu.edu/instrument/filters/data/

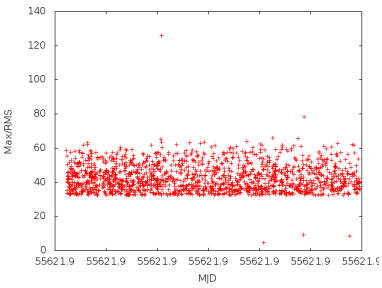

Fig. 2. Selected GPs from WSRT observations from March 1th 2011

sion power of this region was determined via several steps. The energy distribution of the electrons and positrons emitted by the pulsar can be described by a power law

$$n'(\gamma)d\gamma = K'\gamma^{-q}d\gamma$$

with n being the derivative of the number density per unit energy-interval, the power law index q, the Lorentz factor γ and the deviation of the normalisation coefficient K. The latter one is not constant, but wavelength dependent. From **?** several values of K were derived together with a total energy integrated number density of 2 x 10^{-8} cm^{-3}.
The emitted electrons and positrons from the pulsar move into the nebula which is assumed to have a magnetic field strength of B $\approx 10^{-7}$ T (**?**Oort, 1956). Depending upon their velocities they are urged on circular orbits by Lorentz Force and emit electromagnetic radiation caused by gyration. The power of all electrons and positrons gyrating in the magnetic field of the Crab nebula was determined by multiplying the power of a single relativistically gyrating electron (Longair (2002), Rybicki (1979)) with the number of electrons with the energy E. This results in the total emitted power per unit volume and frequency of:

$$p(f) = \int_0^\infty P(f, \gamma(E))KE^{-q}dE$$

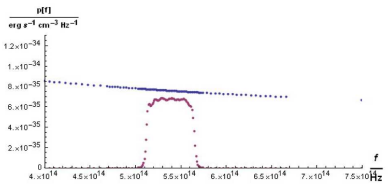

Fig. 3. Spectral power density of an ensemble of electrons and positrons (blue) and with the contribution of the F550M filter (magenta) at optical wavelengths

The normalisation coefficient K was determined in a subsequent computational analysis. To filter out the synchrotron emission at optical wavelengths, border values for the Lorentz factor γ were set. This way and via further numerical calculations of several coefficients the energy distribution of the electrons and protons emitting at optical wavelengths was determined.
Since all discussed HST exposures were taken through the F550M filter, we included its transmittance into the determined energy distribution (Figure 3).
The resulting total synchrotron emission power of an ensemble of electrons and positrons from the anvil region was determined to $P_{em} \approx 10^{33}$ erg s^{-1} while including the filter function the power amounts to $P_{filter} \approx 10^{31}$ erg s^{-1}. The optical emission power was determined to $P_{em} \approx 10^{32}$ erg s^{-1}. It is generally expected that electrons with a power law distribution inherit an energy of $\sim 10^{42}$ erg.

3. Summary

We present a review on the characteristics of radio GPs from the Crab pulsar together with an outlook on the currently ongoing analysis of GPs observed with the WSRT. The initial point of this study is an optical analysis of HST exposures which results in the determination of the synchrotron power output emission value after the Crab flare from September 2010. Examining a possible connection between the recently observed Crab nebula flares and the Crab pulsar, we

search for anomalies in the properties of radio GPs like GP rates, pulse intensity distributions and pulse widths together with a search for changes in the rotation period of the pulsar.

Acknowledgements. The Westerbork Synthesis Radio Telescope is operated by the ASTRON (Netherlands Institute for Radio Astronomy) with support from the Netherlands Foundation for Scientific Research (NWO).
We would like to thank Roy Smith, Gyula Jozsa, Gemma Janssen and the whole Westerbork crew for their essential support in carrying out and processing the radio observations.

References

Abdo et al., Science, 2011, Volume 331 (6018), page 739
Tavani et al.,The Astronomer's Telegram, 2010, 2855
Argyle, E., Gower, J.F.R., Astrophysical Journal, 1972, Volume 175 : page L89
Bilous, A.V., et al., 2009, *Conf. Proc. Fermi Symposium*, C091122
Bilous, A.V., et al., 2010, *Proc. of the ISKAF 2010 Science Meeting, June 10–14*
Bilous, A.V., et al., 2011, ApJ, 728, 110
Hankins, T.H., 2003, Nature, 422 (6928), 141
Hankins, T.H., 2000, in *Proc. of the 177th IAU Coll.*, 202, 165
Hankins, T.H., Eilek, J.A., 2007, ApJ, 670, 693
Hesse, K. H., Wielebinski, R., Astronomy and Astrophysics, 1974, Volume 31 : page 409
Istomin, Y.N., Astronomical Society of the Pacific, 2004, page 369
Jessner, A., et al., 2010, A&A, 524, 60
Jessner, A., et al., 2005, Adv. Space Res., 35 (6), 1166
Karuppusamy, R., Stappers, B., van Straten, W., Astronomy and Astrophysics, 2010, Volume 515 (id.A36)
Kuzmin, A. D., 2007, Ap&SS, 308 (1-4), 563
Longair, M.S., High energy Astrophysics, Cambridge University Press, 2002
Lundgren, S. C., et al., 1995, ApJ, 435, 433
Lyutikov, M., 2007, MNRAS, 381, 1190
Mikhailovskii, A.B., Onishchenko, O.G., Smolyakov, A.I., 1985, Sov. Astr. Lett., 11 (2), 78
Moffett, D.A., Hankins, T.H., 1996, ApJ, 468, 779
Oort, J.H., The Observatory, 1956, Volume 76: page 137-138
Petrova, S.A., 2004, A&A, 424, 227
Popov, M. V., et al., 2006, in *On the Present and Future of Pulsar Astronomy, 26th meeting of the IAU, Joint Discussion 2*
Rybicki, A.P., Lightman, Radiative processes in Astrophysics, John Wiley & Sons 1979
Sallmen, S., Backer, D. C., Hankins, T. H., Moffett, D., Lundgren, S., Astrophysical Journal, 1999, Volume 517 : page 460-471
Shearer, A., et al., 2003, Science, 301, 493
Soglasnov, V., 2007, in *Proc. of the 363 WE-Heraeus Seminar on Neutron Stars and Pulsars 40 years after the discovery*, MPE-Report 291, 68
Slowikowska, A., Jessner, A., Kanbach, G., Klein, B., Proceedings of the 363. WE-Heraeus Seminar on Neutron Stars and Pulsars 40 years after the discovery, 2007, MPE-Report 291: page 64
Staelin, D.H., Reifenstein, E.C., III, 1968, Science, 162 (3861), 1481
Weatherall, J.C., 2001, ApJ, 559, 196